Q FOR 20-SECOND RAYLEIGH WAVES FROM COMPLETE GREAT-CIRCLE PATHS

D. H. von Seggern

Teledyne Geotech

Prepared for:

Air Force Technical Applications Center
Defense Advanced Research Projects Agency

27 February 1975

Unclassified

SECURITY CLASSIFICATION OF THIS PAGE (When Data Entered)

REPORT DOCUMENTATION PAGE		READ INSTRUCTIONS BEFORE COMPLETING FORM
1 REPORT NUMBER SDAC-TR-75-3	2 GOVT ACCESSION NO	3 RECIPIENT'S CATALOG NUMBER
4 TITLE (and Subtitle) Q FOR 20-SECOND RAYLEIGH WAVES FROM COMPLETE GREAT-CIRCLE PATHS		5 TYPE OF REPORT & PERIOD COVERED Technical 6 PERFORMING ORG. REPORT NUMBER
7 AUTHOR(s) von Seggern, D. H.		8 CONTRACT OR GRANT NUMBER(s) F08606-74-C-0006
9 PERFORMING ORGANIZATION NAME AND ADDRESS Teledyne Geotech 314 Montgomery Street Alexandria, Virginia 22314		10 PROGRAM ELEMENT PROJECT, TASK AREA & WORK UNIT NUMBERS
11 CONTROLLING OFFICE NAME AND ADDRESS Defense Advanced Research Projects Agency Nuclear Monitoring Research Office 1400 Wilson Blvd. Arlington, Virginia 22209		12 REPORT DATE 27 February 1975 13 NUMBER OF PAGES ~~30~~ 31
14 MONITORING AGENCY NAME & ADDRESS (if different from Controlling Office) VELA Seismological Center 312 Montgomery Street Alexandria, Virginia 22314		15 SECURITY CLASS (of this report) Unclassified 15a DECLASSIFICATION DOWNGRADING SCHEDULE

16 DISTRIBUTION STATEMENT (of this Report)

APPROVED FOR PUBLIC RELEASE; DISTRIBUTION UNLIMITED.

17 DISTRIBUTION STATEMENT (of the abstract entered in Block 20, if different from Report)

18 SUPPLEMENTARY NOTES

19 KEY WORDS (Continue on reverse side if necessary and identify by block number)

Surface-wave Magnitude
Q
Attenuation of Seismic Waves
Seismic Surface Waves

20 ABSTRACT (Continue on reverse side if necessary and identify by block number)

Seismograms of carefully selected large earthquakes recorded on the high-gain, long-period network were used to visually determine the amplitude ratio of 20-second Rayleigh waves in the R_1 and R_3 phases. Identification of R_3 was aided by applying a time-varying processor which discriminates heavily against ground motion other than the R_3 signal. Ratios were determined in 29 cases representing diverse great circles over the earth; and the average Q estimated for the 20-second, fundamental-mode Rayleigh waves was 498. This

DD FORM 1 JAN 73 1473 EDITION OF 1 NOV 65 IS OBSOLETE

Unclassified

SECURITY CLASSIFICATION OF THIS PAGE (When Data Entered)

value is relevant to distance-amplitude corrections routinely made in M_S calculations and is significantly greater than that Q implied by the current $1.66 \cdot \log\Delta$ relation. Our data did not reveal any significant difference in attenuation over oceanic and continental structures for 20-second Rayleigh waves.

Q FOR 20-SECOND RAYLEIGH WAVES FROM COMPLETE GREAT-CIRCLE PATHS

SEISMIC DATA ANALYSIS CENTER REPORT NO.: SDAC-TR-75-3

AFTAC Project No.: VELA VT/4709

Project Title: Seismic Data Analysis Center

ARPA Order No.: 1620

ARPA Program Code No.: 3F10

Name of Contractor: TELEDYNE GEOTECH

Contract No.: F08606-74-C-0006

Date of Contract: 01 July 1974

Amount of Contract: $2,237,956

Contract Expiration Date: 30 June 1975

Project Manager: Royal A. Hartenberger
(703) 836-3882

P. O. Box 334, Alexandria, Virginia 22314

ib

ABSTRACT

Seismograms of carefully selected large earthquakes recorded on the high-gain, long-period network were used to visually determine the amplitude ratio of 20-second Rayleigh waves in the R_1 and R_3 phases. Identification of R_3 was aided by applying a time-varying processor which discriminates heavily against ground motion other than the R_3 signal. Ratios were determined in 29 cases representing diverse great circles over the earth; and the average Q estimated for the 20-second, fundamental-mode Rayleigh waves was 498. This value is relevant to distance-amplitude corrections routinely made in M_s calculations and is significantly greater than that Q implied by the current $1.66 \cdot \log\Delta$ relation. Our data did not reveal any significant difference in attenuation over oceanic and continental structures for 20-second Rayleigh waves.

ic

TABLE OF CONTENTS

	Page
ABSTRACT	
INTRODUCTION	1
PROCEDURE	5
DATA	7
PROCESSING	11
ANALYSIS	12
RESULTS	19
SUMMARY	21
REFERENCES	22

LIST OF FIGURES

Figure No.	Title	Page
1	Theoretical and empirical diminution with distance for 20-second Rayleigh waves.	2
2	Great-circle paths of 36 signals processed for Q determination: A) Events 1-7, B) Events 8-12.	14
3	Examples of four quality levels of 20-second R_3 identification: A) Type 3 - Very Clear Detection, B) Type 2 - Clear Detection, C) Type 1 - Not Certain Detection, D) Type 0 - No Detection.	15-18

LIST OF TABLES

Table No.	Title	Page
I	Locations of stations in the high-gain, long-period network.	8
II	NOS Parameters for events used in determining Q.	10
III	Results of analysis for Q determination.	13

INTRODUCTION

This report concerns the amplitude-distance relation of Rayleigh waves over the earth, specifically at a period of 20 seconds, because of its importance in the routine seismological excercise of estimating surface-wave magnitudes. This relation can be approximated analytically; provided that the structure is laterally invariant and that frequencies not at an extremum of the group-velocity curve are considered, the time-domain amplitude of seismic surface waves of a given period on a sphere is given by the relation (Sato, 1967):

$$A \propto r^{-\frac{1}{2}} \cdot \sin^{-\frac{1}{2}} \frac{r}{r_e} \cdot \exp \frac{-\pi r}{QUT} \qquad (1)$$

or taking logarithms:

$$\log_{10} A = -\frac{1}{2} \log_{10} r - \frac{1}{2} \log_{10} \left(\sin \frac{r}{r_e} \right) - \frac{\pi r}{QUT} \log_{10} e + k \qquad (2)$$

where r and r_e are the epicentral distance and earth radius in km respectively, Q is the quality factor for absorption, U is the group velocity of surface waves with period T, and k is a constant. The exact rate of diminution of amplitude at a given period is mostly affected by varying Q values since group velocity has a small range of values for a given period greater than 20 seconds, but it is important in assigning surface-wave magnitudes to seismic events to have as good an estimate of the <u>average</u> diminution rate over the earth as possible. Gutenberg (1945) found that observed logarithms of 20-second, Rayleigh-wave amplitudes between 15° and 140° distance could be fit with a straight line of slope $1.656 \cdot \log\Delta$, where Δ is in degrees; that is, a straight line is a good approximation to the terms in equation (2) over this range. The theoretical relation given above and Gutenberg's empirical approximation to it are shown in Figure 1 where a range of Q values has been used for the theoretical calculations. It is apparent that Gutenberg's relation implies a Q of roughly 300 to 350 for Rayleigh waves with periods near 20 seconds. Gutenberg's early relation was confirmed by the Prague conference (Vanek et al., 1962) which, in examining many proposed amplitude-distance relations, found $1.66 \cdot \log\Delta$ to be an average of them; since then the

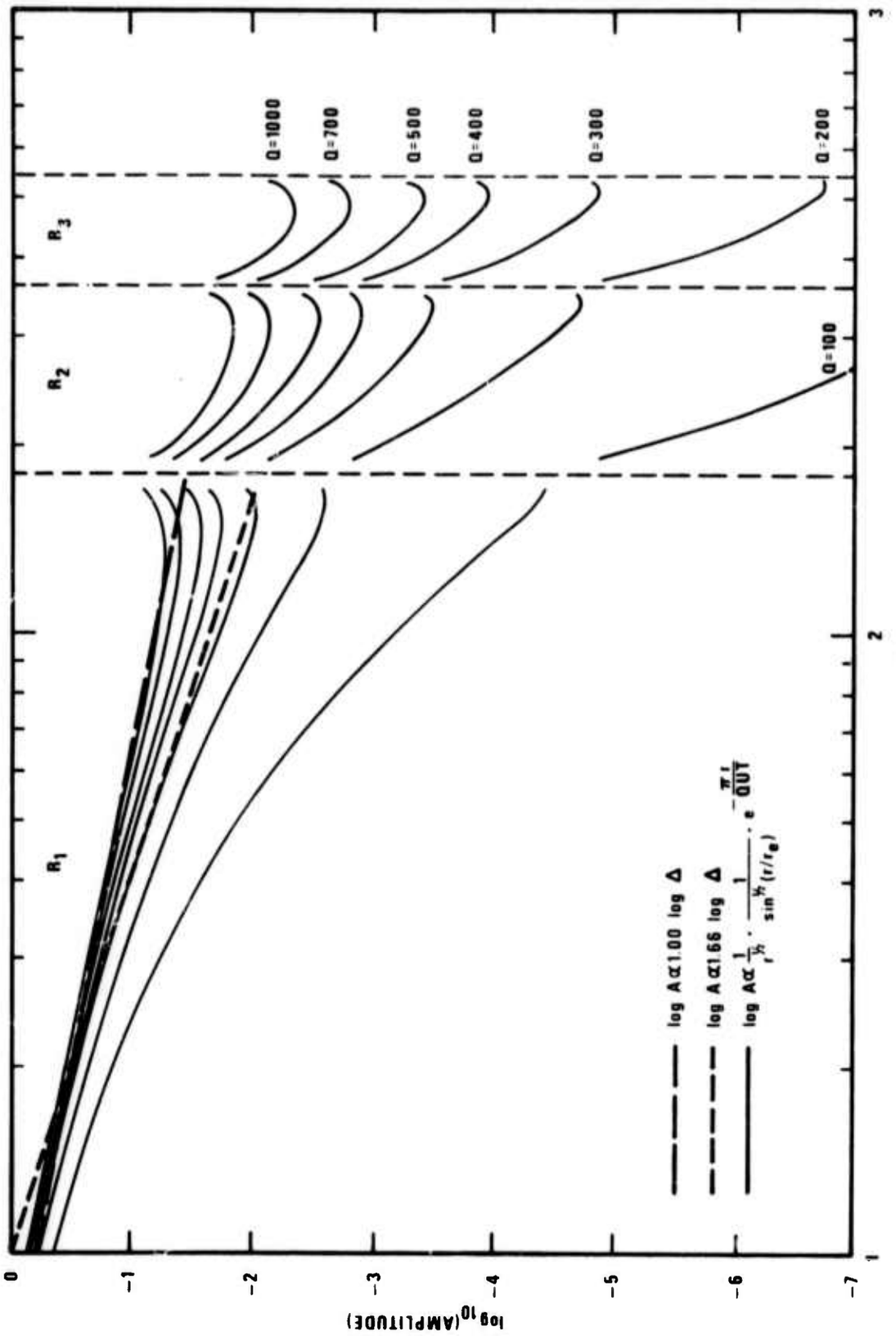

Figure 1. Theoretical and empirical diminution with distance for 20-second Rayleigh waves.

1.66•logΔ relation has been used nearly universally in computing surface-wave magnitudes of seismic events.

In some recent studies, especially with underground nuclear explosion data, it has been found that Gutenberg's relation was improper at regional distances (von Seggern, 1970; Evernden, 1971; Basham, 1971) and that a relation using roughly 1.0•logΔ was better. These problems arose simply because Gutenberg's formula was extrapolated both to distances and to periods less than it was intended for (Alewine, 1972). However, there has been little questioning of its correctness beyond regional distances except for a study (von Seggern, 1975) involving a large data based from 9 stations in the global HGLP (high-gain, long-period) network. That study concludes Rayleigh-wave diminution is well approximated by a 1.0•logΔ relation even out to 140°. This relation is also shown on Figure 1, and it is apparent that it implies a Q on the order of 1000 for Rayleigh waves of 20 seconds.

The purpose of this investigation is to establish a Q for 20-second Rayleigh waves which will reflect a satisfactory sampling of the whole earth and therefore be appropriate as an average Q for this period. Such an estimate will be relevant to improving the amplitude-distance relation for Rayleigh-wave magnitude determination on a routine global basis. We must first briefly review the estimates already published on this parameter. We do so without discussing the possible biases in the studies and the confidence limits on the estimates.

Arkhangelskaya and Fedorov (1961) found Q $\simeq$ 340 for 22-24 sec periods from visual analysis of R_1 and R_2 phases of two earthquakes as recorded at the Moscow station. However, their analysis of R_2 through R_5 amplitudes for the same events gave Q $\simeq$ 1000 for these periods. Tryggvason (1965) used several WWNSS stations and one explosion on Novaya Zemlya to compute spectral amplitudes and thus Q for a wide range of frequencies; his result for 20-sec Rayleigh waves was Q $\simeq$ 1300. Marshall and Carpenter (1966) estimated Q $\simeq$ 400 for 20-sec Rayleigh waves using visual measurements on a suite of recordings in the Northern Hemisphere from Novaya Zemlya explosions. Burton (1974) obtained Q $\simeq$ 380 at 20 sec from Rayleigh-wave spectral calculations at many WWNSS stations for Novaya Zemlya and Lop Nor explosions. Tsai and Aki (1969) obtained Q $\simeq$ 500 at 20 sec from the same type of analysis on an earthquake,

with Q approaching 1000 for periods near 22 sec. To illustrate the elusive nature of the parameter we seek, 20-sec Q for Rayleigh waves, we point to estimates of it ranging from almost 100 to 2000 for the United States from spectral calculations in Solomon (1972), Herrman (1973), and Mitchell (1973).

Certainly, no narrow data base or regional study such as those mentioned here will provide a Q estimate that will be representative of the earth as a whole; furthermore, one is unsure about how to average all the presently available Q estimates. Thus a comprehensive study with new data was desirable.

PROCEDURE

Our approach to the problem will be to estimate the 20-sec Rayleigh-wave Q using the phases R_1 and R_3, and we will do this with visual amplitude measurements. The appropriate relation is

$$Q = \frac{2\pi^2 r_e}{UT\left[\left(\ln(A_1/A_3) - \frac{1}{2}\ln\left(1 + \frac{2\pi r_e}{r}\right)\right)\right]}. \qquad (3)$$

This is derived by writing equation (1) for both R_1 amplitude A_1 and R_3 amplitude A_3, taking the ratio, and solving for Q. Note that the geometric spreading factor $\sin^{-1/2}(x)$ cancels for a complete circuit of the earth. Although this approach is the same as Arkhangelskaya and Fedorov used in a more limited study, we have added some refinements to make our results more robust. The validity of our Q estimate will be based on: 1) using large events, 2) examining many great circle paths around the earth, 3) isolating and enhancing the R_3 phases, and 4) certifying that no signals from aftershocks or other events are masquerading as R_3 phases. Visual measurement is deemed to be as good a procedure as spectral measurements in this case because only one definite period is being considered, Fourier transformation being an unnecessary step. The difference between a spectral estimation and a visual estimation is merely the dispersion factor in (1), $r^{-1/2}$, which comes from the stationary-phase approximation for a travelling surface wave (Sato, 1967). This factor disappears in the case of spectrally-determined amplitudes. Also, in the case of spectral estimation, there is always the problem of window length; for the 20-second amplitude estimate will vary with this length in an undefinable manner. In conclusion there appears to be no real advantage to spectral estimation over simple visual measurement.

It is certain here that we are mostly concerned with amplitudes given by the stationary-phase approximation, appropriate to periods not near an extremum of the group-velocity curve, rather than amplitudes given by the Airy-phase approximation with its corresponding $r^{-1/3}$ factor, appropriate to periods near an extremum; for oceanic group-velocity curves for fundamental-mode Rayleigh waves have no extremum near 20 seconds and only a few particular continental

ones do. Paths considered in this study are 50% to 80% oceanic, and so the dispersion factor for 20-second amplitudes must be $r^{-1/2}$ for most of each great-circle circuit.

DATA

Data for this study was taken exclusively from stations of the HGLP (high-gain, long-period) network. The locations of the eleven stations in this network are given in Table I. Recordings from these instruments have magnifications typically ten times greater than WWNSS long-period instruments due to a shift in the instrument response to longer periods, rigid environmental control, and installation at depth. The three-component instrument outputs are also digitally recorded at a rate of one sample per second.

The choice of events was governed by several criteria. Firstly, they needed to be large enough to generate visible coda 3 to 4 hours after arrival of R_1; this gave high confidence that the phase R_3 was detectable and identifiable at stations. Secondly, they needed to be small enough that quality control, timing, and calibration of the digital traces could be carried out by use of the paper recordings. These criteria translated to events of $m_b \simeq 6$ or $M_s \simeq 6$, for which most body-wave phases were readable but most R_1 amplitudes exceeded the available width on the paper seismograms. Thirdly, events were chosen only if no aftershocks in the 3-4 hour period after R_1 were reported on available epicenter lists. Fourthly, a global distribution of epicenters was desired; that is, many redundant observations due to nearby epicenters was to be avoided.

Point (3) above is a crucial requirement; and clearly the epicenter lists must be complete down to magnitude 4 if we are to be sure that no aftershocks are responsible for erroneous R_3 picks when a R_1/R_3 ratio of roughly 100 is assumed. However, the C-list threshold is near $m_b \simeq 5$ globally while the LASA and NORSAR thresholds are $m_b \simeq 4$ only for small parts of the globe. We therefore sought to eliminate the aftershock uncertainty by checking short-period recordings of available stations closest to the epicenters chosen. For each event we verified that no aftershocks were present at a time which might allow an R_1 from the smaller aftershock to be mistaken for R_3 of the main shock. We augmented this short-period analysis with long-period match filtering of time windows for R_3 using the R_1 of the main shock. This cross-correlation procedure (Capon et al., 1969) should definitely identify within

TABLE I

Locations of Stations in the
High-Gain, Long-Period Network

Station	Location	Latitude	Longitude	Vertical-Component Magnification (1972)
ALQ	Albuquerque, New Mexico	34.9N	106.5W	100,000-120,000
CHG	Chiang Mai, Thailand	18.8N	99.0E	66,000
CTA	Charters Towers, Australia	20.1S	146.2E	125,000
EIL	Eilat, Israel	29.5N	34.9E	40,000-100,000
FBK	Fairbanks, Alaska	64.9N	148.0W	37,000
KIP	Kipapa, Hawaii	21.4N	158.0W	55,000
KON	Kongsberg, Norway	59.7N	9.6E	114,000
MAT	Matsushiro, Japan	36.5N	138.2E	40,000
OGD	Ogdensburg, New Jersey	41.1N	74.6W	80,000
TLO	Toledo, Spain	39.9N	4.0W	76,000
ZLP	La Paz, Bolivia	16.3S	68.1W	94,000

the R_3 window any R_1 from an aftershock or from an unrelated event within a few hundreds of kilometers from the epicenter of the main shock.

Twelve events meeting the above criteria were selected for processing and are listed in Table II. The choice of stations for each event was made on the basis of availability and data quality; over one-half of the possible event-station combinations were unable to be processed due to station down time on one or more components or inability to retrieve the digital data from the tapes. Some other combinations were eliminated when visual analysis showed that coda amplitude to be below normal background noise level within 3 to 4 hours after R_1; these noise levels varied by nearly an order of magnitude. R_1 itself was often lower in these cases due most likely to radiation pattern. So for these cases a combination of source effects and station noise, not necessarily high attenuation for R_3, made them unsuitable for this study.

TABLE II

NOS Parameters for Events Used in Determining Q

Event No.	Date	Origin Time	Latitude	Longitude	Depth	m_b	M_s	Geographic Region
1	7 Jan 72	06:25:48	2.1S	139.0E	33	5.9	5.9	Near N. Coast of West New Guinea
2	20 Mar 72	07:33:50	6.8S	76.8W	64	6.1	-	Northern Peru
3	20 Mar 72	23:31:49	51.3N	179.2W	46	6.0	5.4	Andreanof Islands, Aleutian Islands
4	02 May 72	06:56:23	5.2N	100.3W	33	5.8	5.5	East Central Pacific Ocean
5	04 May 72	21:40:01	35.1N	23.6E	46	5.9	6.3	Crete
6	05 May 72	23:16:28	4.1S	152.7E	32	5.6	6.6	New Britain Region
7	12 Jun 72	19:47:37	53.3N	166.8W	44	5.8	5.8	Fox Islands, Aleutian Islands
8	24 Jun 72	15:29:22	36.2N	69.7E	47	6.0	6.1	Hindu Kush Region
9	27 Sep 72	09:01:44	16.5S	172.2W	33	5.9	6.0	Samoa Islands Region
10	30 Oct 72	16:48:09	6.3S	154.8E	50	5.8	6.2	Solomon Islands
11	10 Dec 72	18:26:07	44.8N	149.4E	13	6.0	5.8	Kurile Islands
12	22 Jun 73	00:37:58	18.6N	105.0W	33	5.6	6.1	Off Coast of Jalisco, Mexico

PROCESSING

The three components of the 36 qualifying seismograms were calibrated relative to one another and rotated into components parallel and transverse to the great circle path, with the vertical component unchanged. Then a Rayleigh-wave enhancer as described by Simons (1968) was applied to the entire time interval from the start of R_1 past the expected time of arrival of 20-second R_3. This time-varying signal enhancer operates in the frequency domain to eliminate harmonic components not of the desired Rayleigh-wave type. It discriminates against ground motion which is Rayleigh waves but off the great circle path by a factor equal to $\cos^4\alpha$ where α is the difference between the observed and computed back azimuth. Cases where R_1 arrives at angles significantly off the back azimuth are not unusual; and it is expected that for R_3, which travels an additional full circuit of the earth, these cases would be more common and certainly more severe. So, even though we are discriminating against signals from other azimuths, we may be attenuating the R_3 phase itself somewhat; and so our Q estimates will be biased to the low side. Also, the processor discriminates against harmonic components not having the Rayleigh-wave particle motion by a factor equal to $\cos^8\beta$ where β is the difference between the observed phase angle of the vertical relative to the radial recording and the required phase angle of $\pi/2$. Since the presence of considerable noise in the R_3 window should cause deviations in this angle, we expect some further attenuation of the R_3 phase; and this will further bias our Q estimates to the low side.

ANALYSIS

Results of individual analysis of the 36 processed seismograms are presented in Table III. Both R_1 and R_3 amplitudes were measured on the processor outputs for the vertical component. The critical stage of the analysis was the identification of the R_3 phase having periods near 20 seconds. This identification was aided by checking the group velocity indicated by the 20-second R_1-R_3 time delay against expected group velocity based on the structure of the complete great circle path. These predicted paths are shown in Figure 2. Percentages of oceanic and continental structure were measured in each case; and using 3.8 km/sec for the former and 3.0 km/sec for the latter, we calculated the expected travel time and average group velocity for each case. The observed group velocities are listed in Table III; recognizing that significant departures from the great circle path might occur for R_3, we accepted as valid some R_3 arrivals which were considerably earlier or later than expected, where observed group velocity was up to 0.2 km/sec different from that expected. Identification of R_3 arrivals in the 20-second period range was also frequently aided by visibility of the entire R_3 phase, smoothly dispersed from a longer-period Airy phase down through shorter periods below 20 seconds.

The 20-second R_3 phases were graded as indicated in Table III from 0 to 3 according to the quality or confidence of the observation. Quality "3" indicated a 20-second R_3 which is unmistakable at even a casual glance; if so graded, the phase is most often identifiable on the unprocessed seismogram and is part of a plainly dispersed R_3 wave train. Quality "2" indicates an R_3 which is identifiable only after processing; some examination of the seismogram is required to establish its validity, but it is certainly felt to be a correct pick. Quality "1" indicates an R_3 of uncertain validity; these phases were identified only after careful consideration of all relevant data, and there is no clearly dispersed wave train. Quality "0" indicates an R_3 could not be identified; either noise obscured it or its angle of approach was so different from the back azimuth to the epicenter that the time-varying adaptive processor attenuated it severely. An example of each of the four qualities is shown in Figure 3.

TABLE 1II

Results of Analysis for Q Determination

Event No.	Station	Epicentral Distance(km)	Back Azimuth	Percentage Oceanic Path	Group Velocity (km/sec)	R_3 Detection Quality	Amplitude Ratio A_1/A_3	Q	Comments
1	OGD	14,540	313°	80%	3.61	3	101.	440	
2	EIL	12,438	275°	51%	3.60	1	502.	317	early arrival
2	FBK	9,816	110°	41%	-	0	-	-	noisy
2	TLO	9,043	254°	49%	3.42	2	169.	429	early arrival
3	FBK	2,344	245°	72%	3.41	2	96.7	589	late arrival
3	KON	7,698	6°	64%	3.32	2	129.	479	late arrival
3	TLO	9,906	357°	69%	-	0	-	-	noisy
4	ALQ	3,347	168°	55%	3.26	1	483.	393	late arrival
4	CTA	12,652	93°	72%	-	0	-	-	noisy - no 20-sec at all
4	KIP	6,459	97°	79%	-	0	-	-	noisy
4	KON	10,613	290°	71%	3.44	1	254.	384	low amplitude
5	KIP	13,765	358°	73%	3.42	3	116.	451	
6	CTA	1,900	22°	69%	3.57	3	22.8	1108	
6	KIP	6,062	248°	73%	3.53	3	48.9	618	
6	KON	13,102	43°	71%	-	0	-	-	signal off great circle path
7	CTA	9,292	26°	75%	3.64	2	32.	656	
7	KIP	3,619	350°	49%	3.34	3	495.	379	
7	KON	7,497	358°	62%	3.53	2	63.2	553	
7	OGD	6,625	316°	81%	3.50	3	111.	481	
8	KIP	11,909	321°	58%	3.21	1	376.	377	late arrival
8	KON	4,966	94°	77%	3.48	3	220.	421	
8	OGD	10,719	28°	64%	3.57	2	245.	373	early arrival
9	ALQ	8,959	242°	65%	3.51	3	191.	407	
9	KIP	4,465	201°	56%	3.31	3	141.	500	
9	KON	15,228	2°	67%	-	0	-	-	strong microseisms
10	KIP	5,988	245°	74%	3.57	3	150.	441	
10	KON	13,410	41°	75%	3.37	2	94.0	484	late arrival
11	CHG	5,459	47°	79%	3.61	1	298.	375	
11	KIP	5,434	311°	69%	3.39	3	303.	398	
11	KON	7,878	29°	57%	3.59	2	90.5	485	early arrival
11	ZLP	15,299	320°	59%	3.32	1	406.	353	
12	CHG	15,122	34°	70%	-	0	-	-	noisy
12	KIP	5,526	83°	69%	3.50	3	102.	503	
12	KON	9,548	300°	67%	3.46	2	271.	380	
12	MAT	11,011	59°	74%	3.50	2	166.	413	
12	ZLP	5,583	312°	80%	3.63	2	338.	363	

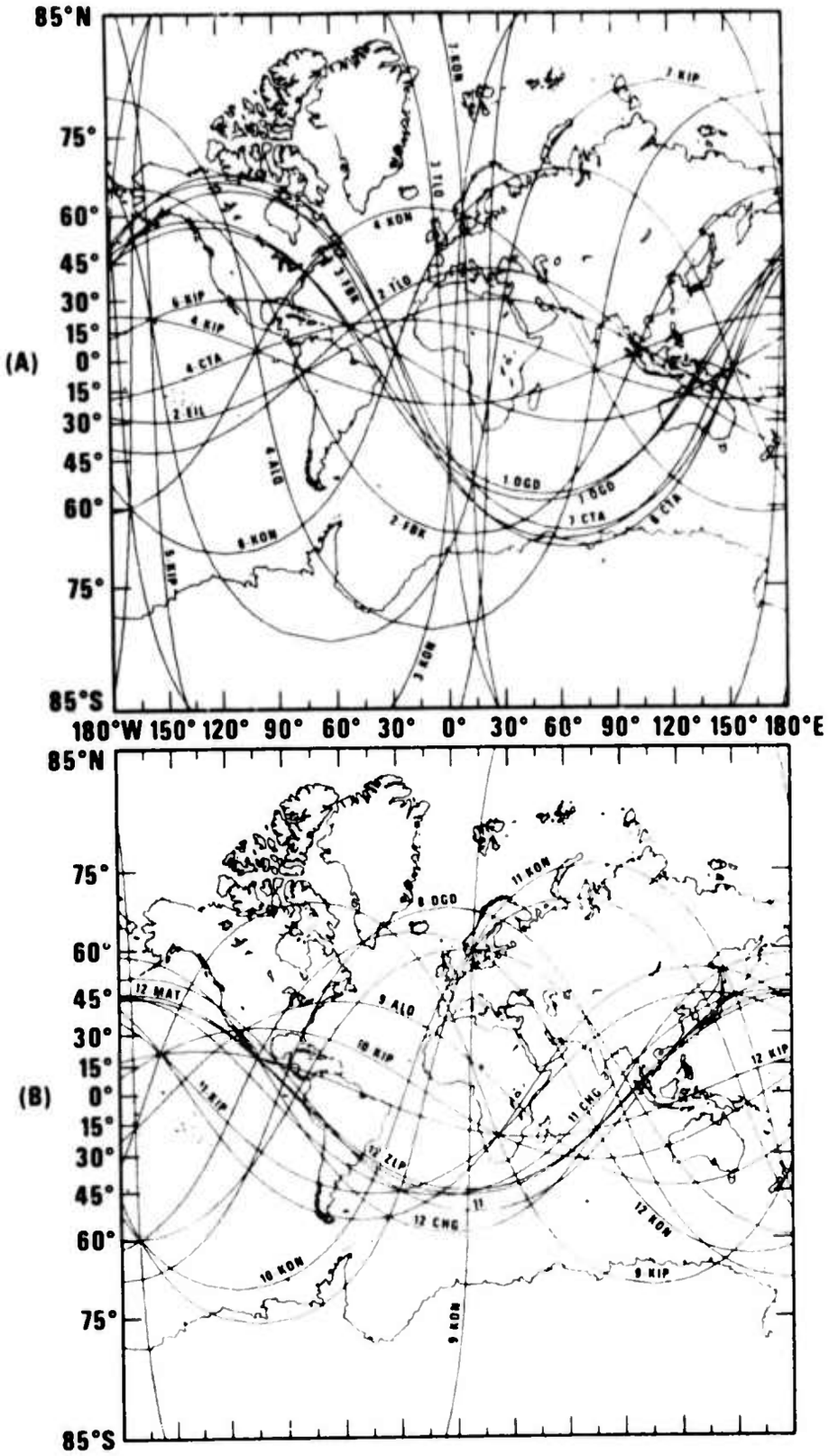

Figure 2. Great-circle paths of 36 signals processed for Q determination: A) Events 1-7 , B) Events 8-12.

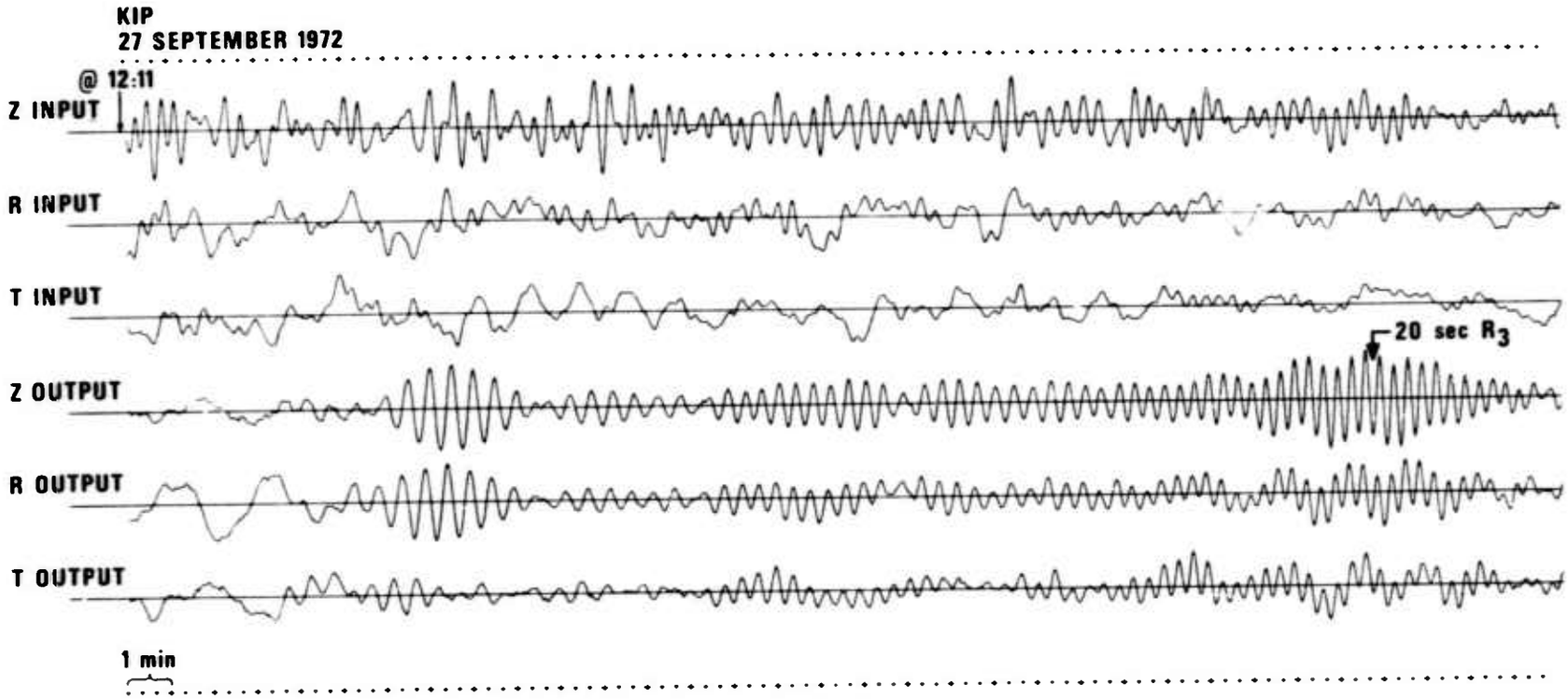

A) Type 3 - Very Clear Detection

Figure 3. Examples of four quality levels of 20-second R_3 identification.

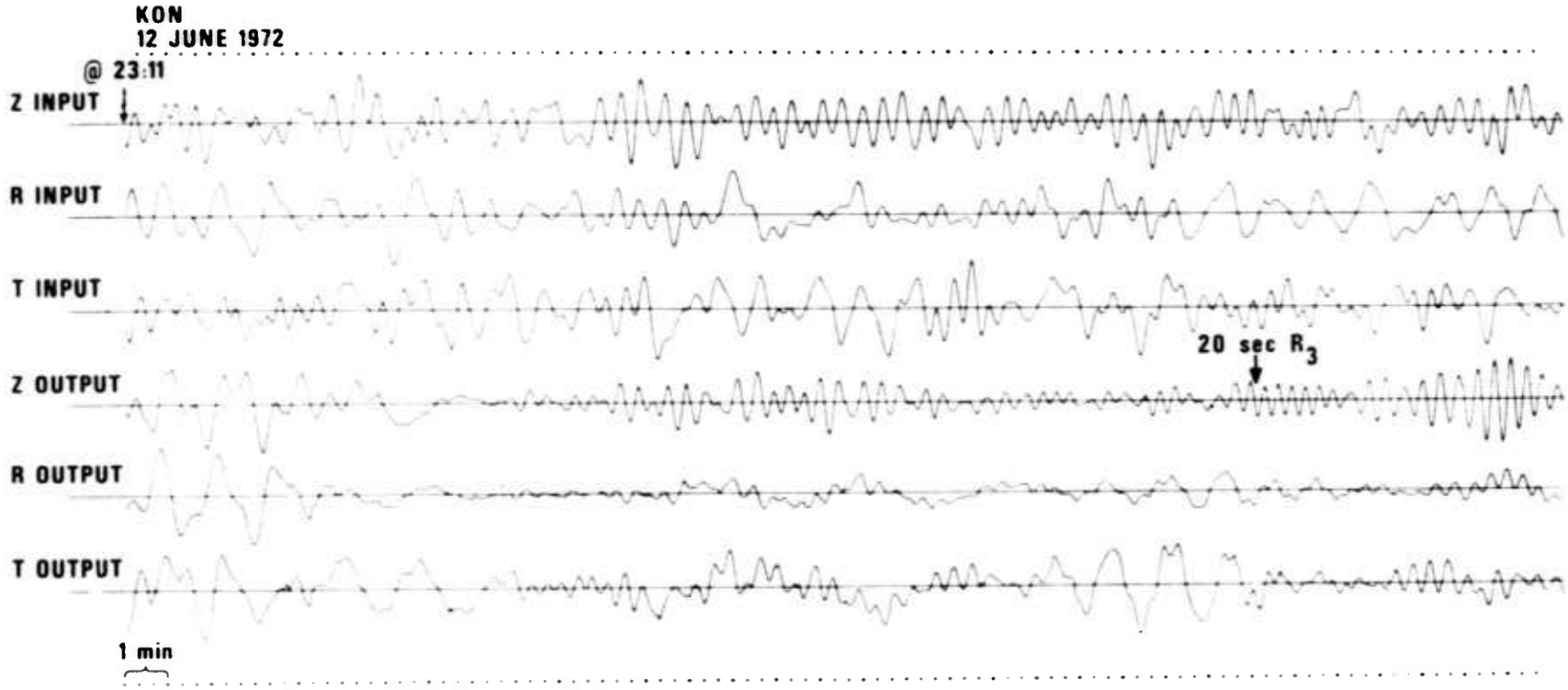

Figure 3 (Cont.) B) Type 2 - Clear Detection

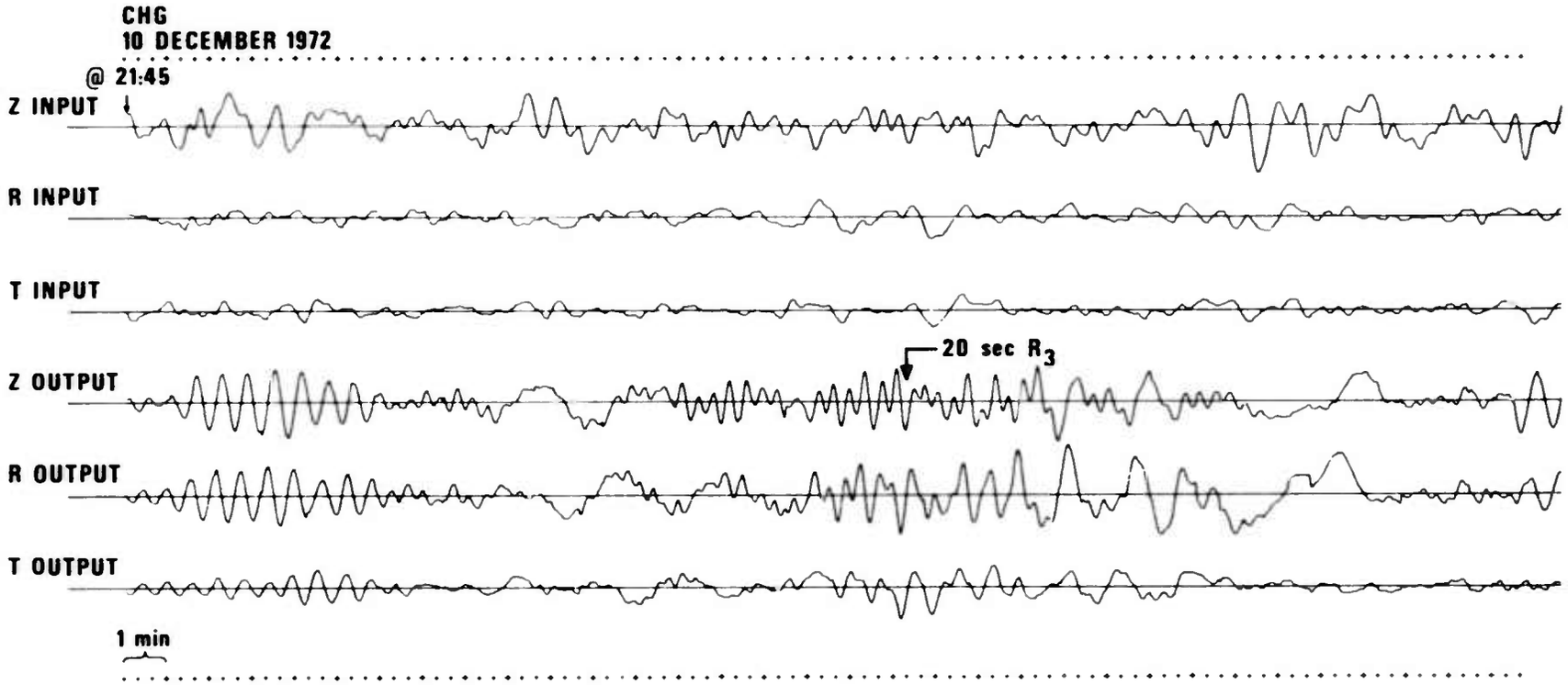

Figure 3 (Cont.)

C) Type 1 - Not Certain Detection

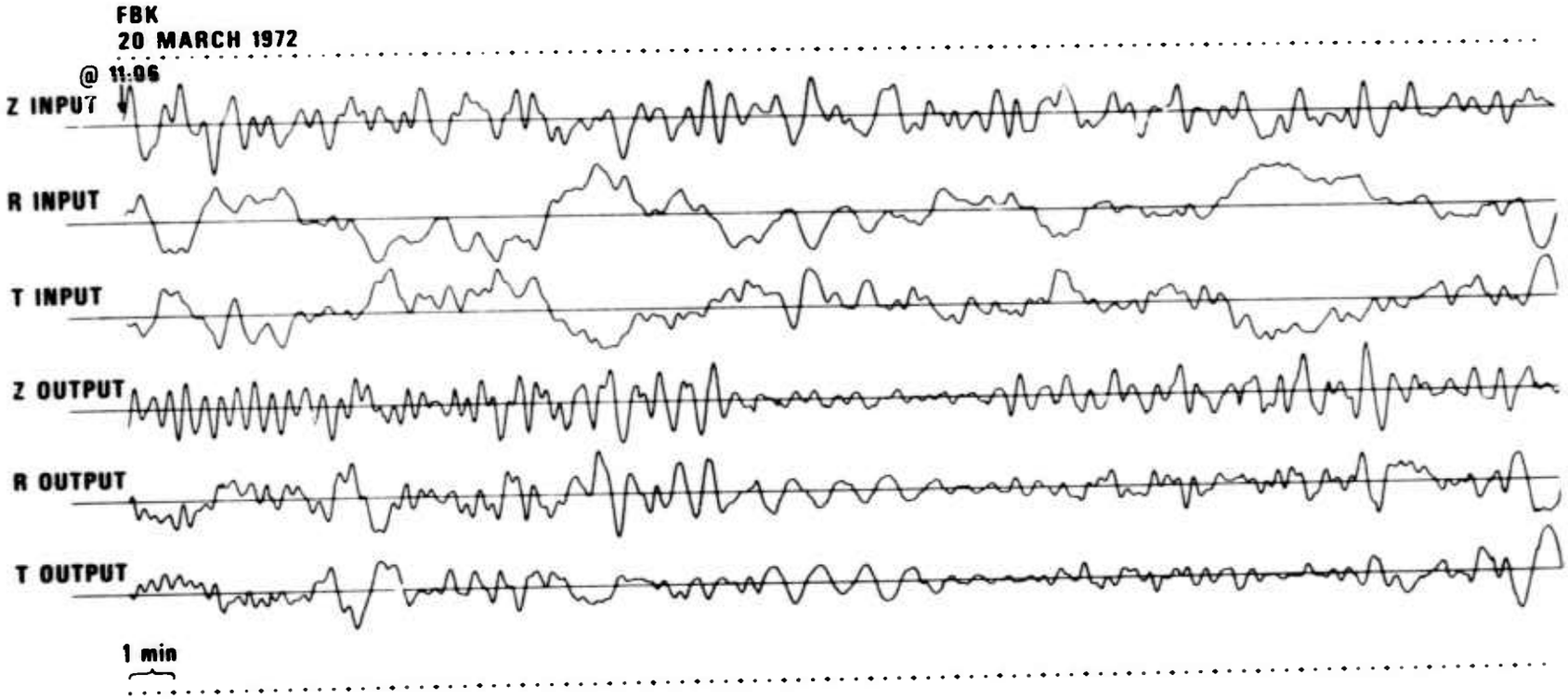

Figure 3 (Cont.)

D) Type 0 - No Detection

RESULTS

The Q values in Table III were calculated according to equation (3). Assuming the amplitude ratios A_1/A_3 to have log-normal distribution, the individual 1/Q estimates would be normally distributed. On this basis the mean and 90% confidence limits for 1/Q were then calculated and inverted, giving $\overline{Q} = 441$ and $408 < \overline{Q} < 478$. These confidence intervals are not meaningful except to indicate the scatter of the data because we have already explained that our average Q estimate will be biased low due to the processor attenuating R_3 more than R_1. In order to establish quantitatively how great this bias might be, we reexamined the phases on those recordings having quality 3 identifications of R_3. In 10 of the 12 cases, R_3 was reliably measurable on the unprocessed trace by simply correlating the motion before and after processing; in other words, noise was little or no hindrance. With R_1 also remeasured on the unprocessed trace, we were able to form A_1/A_3 ratios for the raw data; these ratios were uniformly lower than these presented in Table III for the processed data by a factor of between one-fourth and one. The average factor over the 10 cases was .63; assuming this is a rough empirical correction factor for all A_1/A_3 ratios in Table III, a corrected set of 29 ratios was used to obtain $\overline{Q} = 498$. We regard this as the more accurate estimate.

Since we have graded the R_3 identifications, it is tempting to delete the lesser quality R_1/R_3 ratios, flagged as 1 in Table III, and recompute the average Q. But, noting that these ratios in Table III result in the lowest Q's generally, for high attenuation paths we regard these as valid estimates which should be equally weighted in computing the mean Q over the globe. For those seven cases where no R_3 was identified, and thus where attenuation might be considered to be greatest, an upper bound for R_3 amplitude can be set by measuring the largest 20-second cycle; Q's calculated on this basis though were not generally low. We feel that in these seven cases, the inability to identify R_3 is due as much to high noise or to propagation far off the back azimuth as to low Q; and we refrain from using these noise amplitudes to make a Q estimate.

Since we have already estimated the percentage of oceanic and continental structure in each path, it is desirable to test whether our data indicates any

significant difference between oceanic and continental attenuation. To derive the necessary regression equation, manipulate equation (3) to get:

$$\frac{T}{\pi}\left(\ln\left(\frac{A_1}{A_3}\right) - \frac{1}{2}\ln\left(1 + \frac{2\pi r_e}{r}\right)\right) = \frac{2\pi r_e}{QU}$$

Separate the right-hand side into oceanic and continental terms thus:

$$\frac{T}{\pi}\left(\ln\left(\frac{A_1}{A_3}\right) - \frac{1}{2}\ln\left(1 + \frac{2\pi r_e}{r}\right)\right) = \frac{1}{Q_o}\frac{r_o}{U_o} + \frac{1}{Q_c}\frac{r_c}{U_c}$$

where $r_o + r_c = 2\pi r_e$, the total circumference of the earth. We set T = 20 second U_o = 3.8 km/sec, U_c = 3.0 km/sec and solve for the regression conefficients $\hat{Q}_o^{-1}$ and $\hat{Q}_c^{-1}$ by least squares procedure. The results were inverted to get $\hat{Q}_o$ = 527 and $\hat{Q}_c$ = 341. A statistical test for identify of Q_o and Q_c, assuming $\hat{Q}_o^{-1}$ and $\hat{Q}_c^{-1}$ to be random normal estimators of the same Q^{-1}, showed that the difference $(\hat{Q}_c^{-1} - \hat{Q}_o^{-1})$, and thus the difference between $\hat{Q}_c$ and $\hat{Q}_o$, was significant at only the 59% confidence level. Use of corrected A_1/A_3 ratios, as explained above, results in $\hat{Q}_o$ = 618 and $\hat{Q}_c$ = 406 with the difference being significant at only the 60% confidence level. We cannot then reject the possibility that $Q_o = Q_c$. Gutenberg (1945) and Tsai and Aki (1969) report $Q_o < Q_c$, but in these studies the data is insufficient also to establish the relation between continental and oceanic attenuation with high confidence. The main impediment to establishing this relation to a high degree of confidence with our data is that the percentages of oceanic versus continental path as seen in Table III are not greatly different, ranging from fifty to eighty percent oceanic, so that very little of the data scatter can be accounted for by differences in Q between the two structures. Also, we know that the Rayleigh waves examined will certainly travel paths different from the great circle path through the epicenter and station and that thus our estimated percentage of oceanic path in Table III will be a rough approximation, possibly being quite erroneous in some cases.

SUMMARY

Use of large, carefully selected earthquakes, the HGLP network of seismic stations, and simple digital processing of seismograms enabled us to routinely detect shorter periods of the R_3 phase. Amplitude ratios of these and associated R_1 phases at 20 seconds' period provided Rayleigh-wave Q estimates for 29 different, full great-circle paths on the globe. These empirical Q estimates include the effects of reflections, refractions, focusing - defocusing, mode conversion, and scattering as well as intrinsic absorption; therefore they are relevant to determining standardized Rayleigh-wave distance-correction terms for calculation of M_s of worldwide seismic events. Data of this paper resulted in an overall Q of 498, a value which would predict diminution of 20-second Rayleigh waves to be significantly less than that implied by the accepted $-1.66 \log\Delta$ relation for amplitude. Our data was insufficient to show whether there is a difference between oceanic and continental paths in regard to attentuation of 20-second Rayleigh waves.

Although our interest lay in the 20-second periods, the data for other periods such as 40 seconds could easily be gleaned by reexamining the processed seismograms. In fact, the entire dispersed R_3 phase was vividly clear in some cases after application of the time-varying processor for Rayleigh-wave enhancement; and some features of interest for further studies appeared, such as multipath arrivals for 60-80 second Airy phases.

REFERENCES

Alewine, R. W., 1972, Theoretical and observed distance corrections for Rayleigh-wave magnitude, Bull. Seismol. Soc. Amer., v. 62, p. 1611-1619.

Arkhangelskaya, V. M., and S. A. Fedorov, 1961, Damping of surface Rayleigh waves, Izvestiya, Geophysics Series, No. 8 (1961), p. 738-743 (English translation).

Basham, P. W., 1971, A new magnitude formula for short-period continental Rayleigh waves, Geophys. J. Roy. Astr. Soc., v. 23, p. 255-260.

Burton, P. W., 1974, Estimations of Q_γ^{-1} from seismic Rayleigh waves, Geophys. J. Roy. Astr. Soc., v. 36, p. 167-189.

Capon, J., R. J. Greenfield, and R. T. Lacoss, 1969, Long-period signal processing results for the Large Aperature Seismic Array, Geophysics, v. 34, p. 305-329.

Evernden, J. F., 1971, Variation of Rayleigh-wave amplitude with distance, Bull. Seismol. Soc. Amer., v. 61, p. 231-240.

Gutenberg, B., 1945, Amplitudes of surface waves and magnitudes of shallow earthquakes, Bull. Seismol. Soc. Amer., v. 35, p. 3-12.

Herrmann, R. B., 1973, Surface-wave generation by the south-central Illinois earthquake of November 9, 1968, Bull. Seismol. Soc. Amer., v. 63, p. 2121-2134.

Marshall, P. D., and E. W. Carpenter, 1966, Estimates of Q for Rayleigh waves, Geophys. J. Roy. Astr. Soc., v. 10, p. 549-550.

Mitchell, B. J., 1973, Radiation and attenuation of Rayleigh waves from the southeastern Missouri earthquake of October 21, 1965, J. Geophys. Res., v. 78, p. 886-899.

Sato, R., 1967, Attenuation of seismic waves, J. Phys. Earth, v. 15, p. 32-61.

Simons, R. S., 1968, A surface wave particle motion discrimination process, Bull. Seismol. Soc. Amer., v. 58, p. 629-638.

REFERENCES (Continued)

Solomon, S. C., 1972, Seismic-wave attenuation and partial melting in the upper mantle of North America, J. Geophys. Res., v. 77, p. 1483-1502.

Tryggvason, E., 1965, Dissipation of Rayleigh wave energy, J. Geophys. Res., v. 70, p. 1449-1455.

Tsai, Y. B., and K. Aki, 1969, Simultaneous determination of the seismic moment and attenuation of seismic surface waves, Bull. Seismol. Soc. Amer., v. 59, p. 275-288.

Vanek, J., A. Zatopek, V. Karnik, N. V. Kondorskaya, Y. V. Riznichenko, E. F. Savarensky, S. L. Solov'ev, and N. V. Shebalin, 1962, Standardization of magnitude scales, Izvestiya, Geophysical Series, No. 2 (1962), p. 108-111 (English translation).

von Seggern, D. H., 1970, Surface-wave amplitude-versus-distance relation in the Western United States, SDL Report No. 249, Teledyne Geotech, Alexandria, Virginia.

von Seggern, D. H., 1975, Distance-amplitude relationships for long-period P and S and for LR from measurements on recordings of the long-period experimental stations, SDAC report in preparation.